Droplet Incubation and Splitting in Open Microfluidic Channels

Samuel B. Berry*[1], Jing J. Lee*[1], Jean Berthier[1], Erwin Berthier[1], Ashleigh B. Theberge[1,2 §]
[1]Department of Chemistry, University of Washington, Box 351700, Seattle, Washington 98195, USA
[2]Department of Urology, University of Washington School of Medicine, Seattle, Washington 98105, USA
*These authors contributed equally to this work
[§]Corresponding author: Dr. Ashleigh Theberge, abt1@uw.edu

The supporting information for "Droplet Incubation and Splitting in Open Microfluidic Channels"" includes additional information that readers might find useful for adapting the open channel systems presented here for their own work; this includes detailed schematics and dimensions of each platform described in this work and corresponding computer aided design (CAD) files, a derivation of the analytical model used to describe flow in the bypass system, an illustrated workflow of the droplet length measuring protocol used for Figure 3D, results demonstrating the reproducibility of droplet splitting in one device, and videos showing the use and function of each platform in this work.

Supporting information contents:

Additional supporting information included:

S1: Droplet Behavior Modes in Open Channel Platform

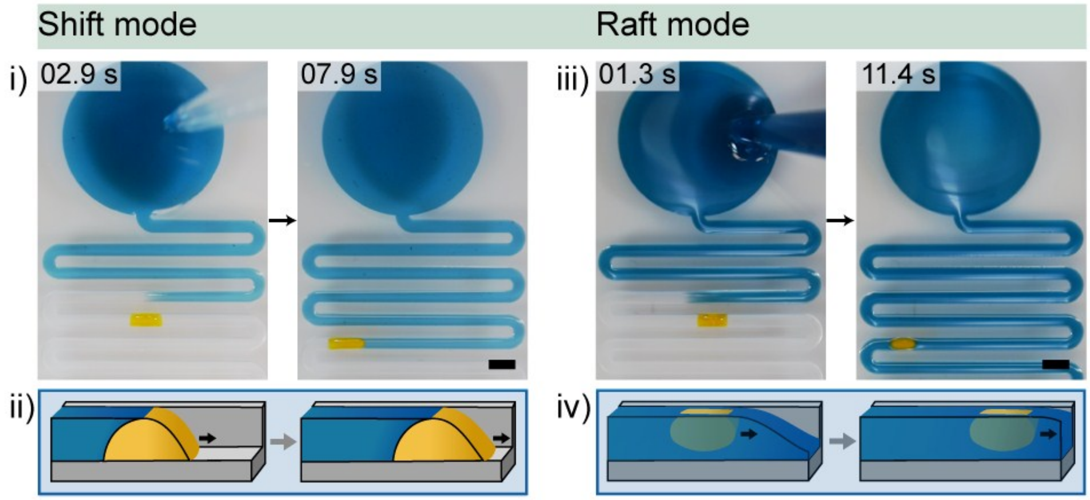

Figure S1: A single static aqueous droplet (yellow) is pipetted into the channel and can display either shift mode ((i) and (ii)) or raft mode ((iii) and (iv)) as carrier fluid (blue) moves the aqueous droplet down channel.[1] For shift mode, the carrier phase is 1-pentanol; for raft mode, the carrier phase is toluene. Scale bar: 2 mm. Schematics in (ii) and (iv) are reproduced from Lee et al.[1] Videos for (i) and (iii) are included (Videos S1 and S2).

Reference:

1. Lee, J.J.; Berthier, J.; Brakke, K.A.; Dostie, A.M.; Theberge, A.B.; Berthier, E. Droplet behavior in Open Biphasic Microfluidics. *Langmuir*, **2018**, 34, 18, 5358-5366.

S2: Detailed Device Schematics and Dimensions

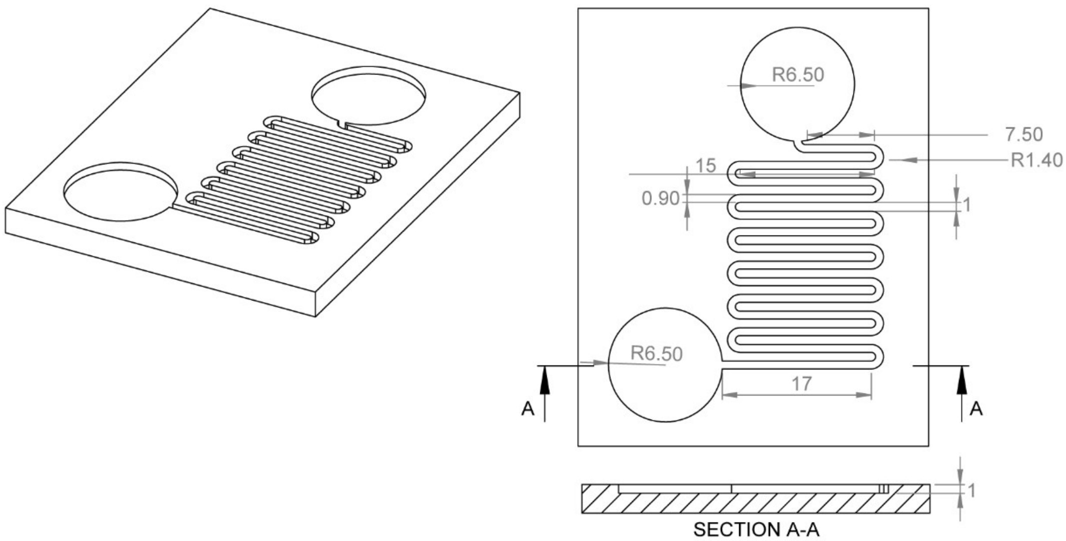

Figure S2i: Detailed device schematics illustrating device dimensions for the Coalescence Device (Figure 2A). Units in mm.

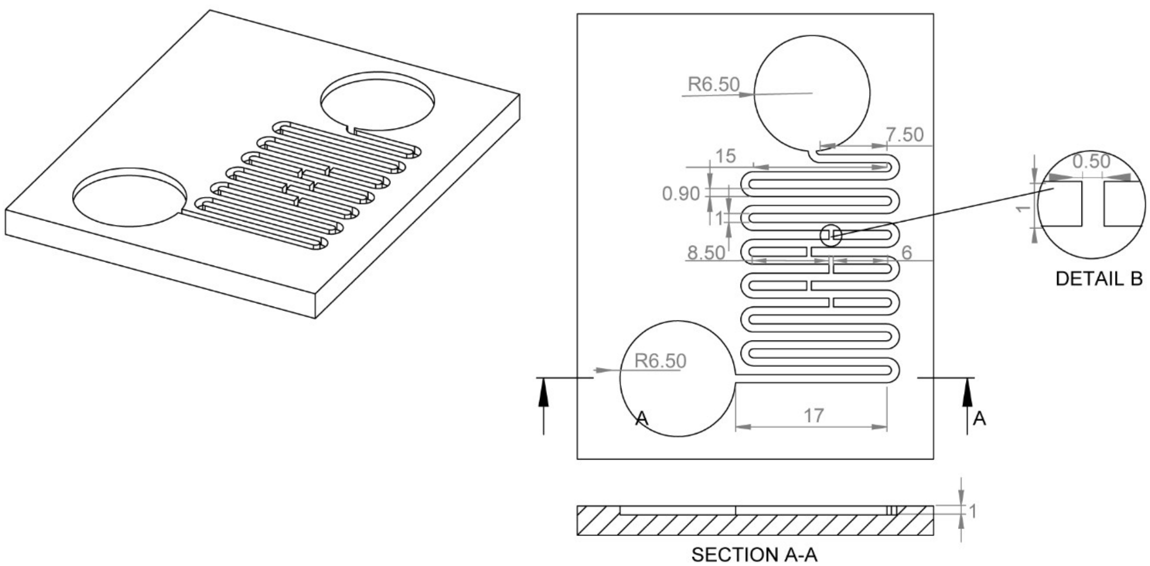

Figure S2ii: Detailed device schematics illustrating device dimensions for the Bypass Device without a step (Figure 2B). Units in mm.

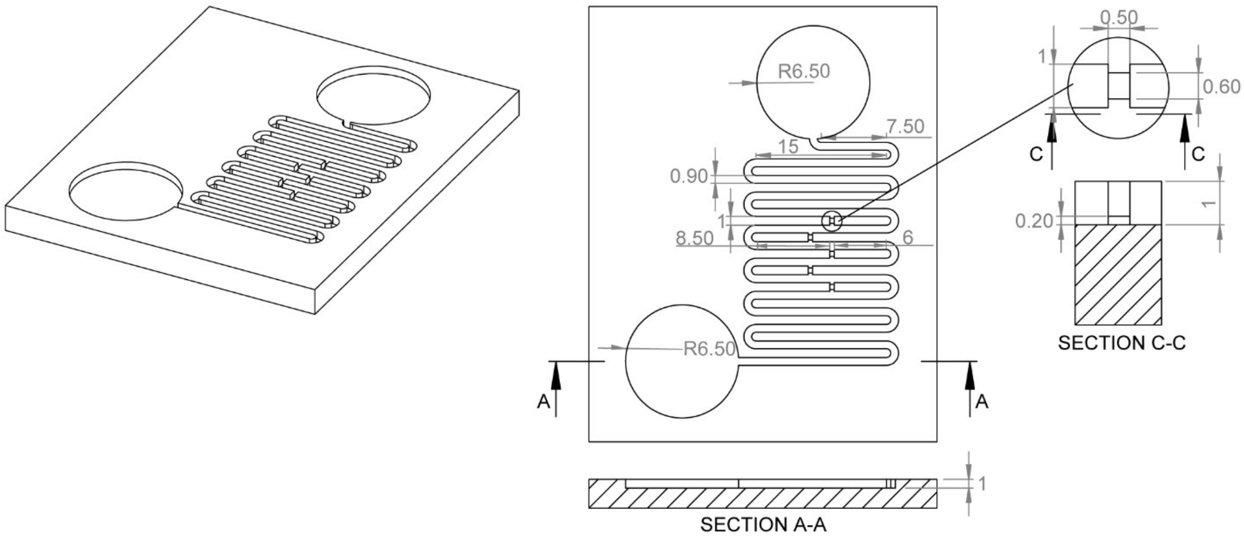

Figure S2iii: Detailed device schematics illustrating device dimensions for the Bypass Device with a step (Figure 2C). Units in mm.

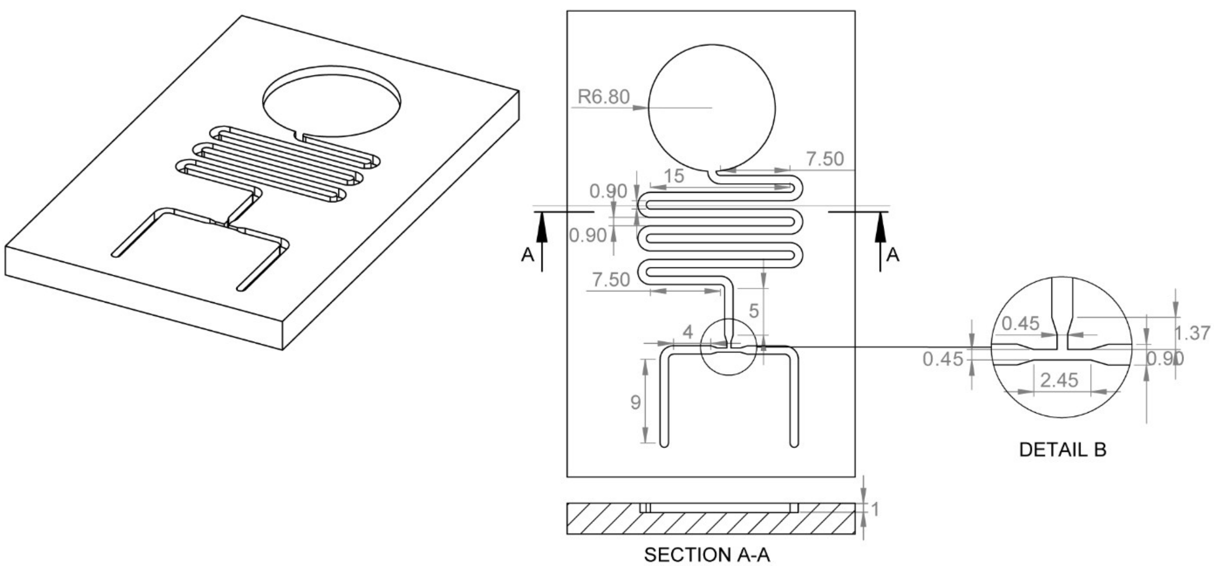

Figure S2iv: Detailed device schematics illustrating device dimensions for the symmetric splitting T junction device (Figure 4B). Units in mm.

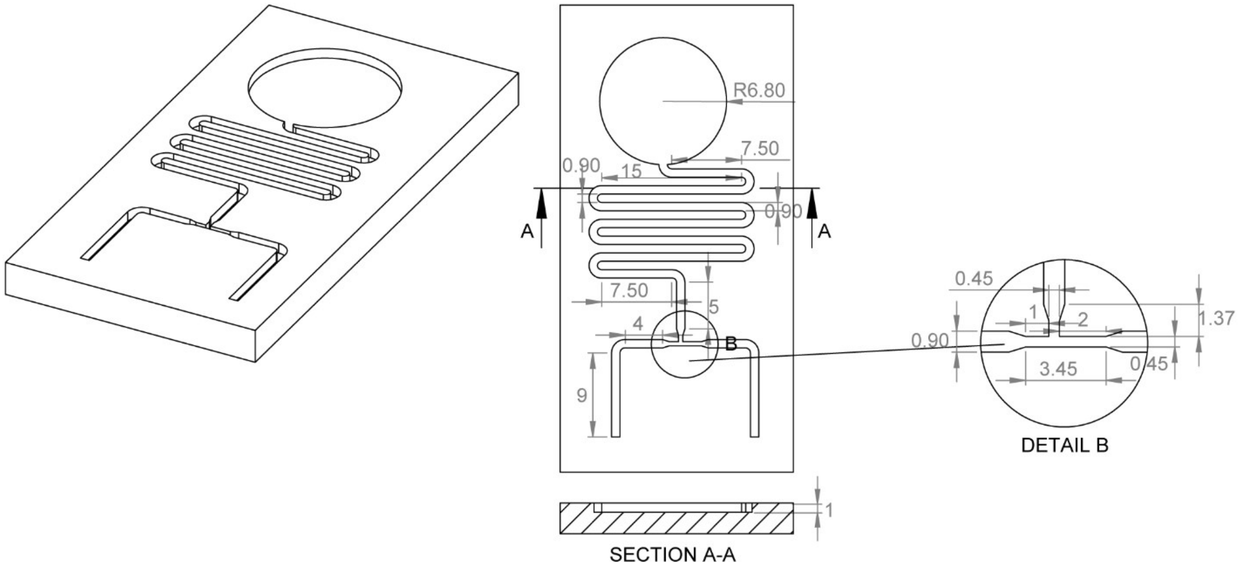

Figure S2v: Detailed device schematics illustrating device dimensions for the asymmetric splitting T junction device (Figure 4C). Units in mm.

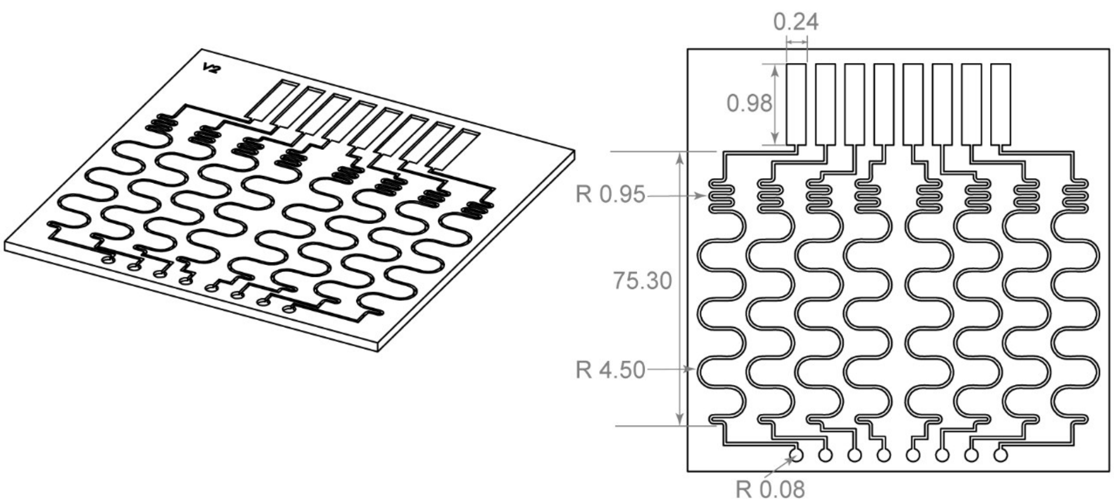

Figure S2vi: Detailed device schematics illustrating device dimensions for the multichannel coalescence device (Figure 3). Units in mm.

S3: Derivation of Analytical Model for Resistance and Flux

In this model, we considered an open channel system with a bifurcation and two nodes, where the flows partition at the first node (green dot) and join at the second (red dot). Between the two nodes are two different branches (blue and yellow outlines); Branch 1 is an extension of the main channel, and Branch 2 is the bypass channel with a step in the middle (Figure S3i).

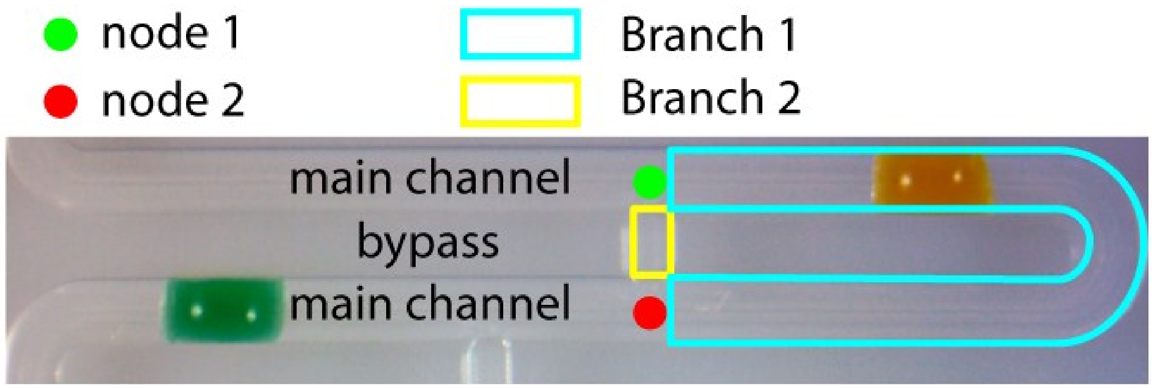

Figure S3i: Labeled top view image of open channel system.

Based on previous work[1] on the creation of a generalized Lucas-Washburn law for varying shapes driven by capillary flow and application of the analogy of an electric circuit, we can write:

$$\Delta P = P_1 - P_2 \approx \tilde{R}_1 Q_1 \approx \tilde{R}_2 Q_2 \tag{1}$$

$$\mu \frac{p}{\lambda S^2} L = R \tag{2}$$

Where P_1 and P_2 are the pressures at node 1 and node 2, respectively, R is the resistance, L is the length, Q is the flux, S is the channel cross sectional area, μ is the liquid viscosity, p is the total perimeter, and λ is the friction length.[2]

Solving equation 1 for Q:

$$\left(\frac{\tilde{R}_1}{\tilde{R}_2}\right) = \left(\frac{Q_2}{Q_1}\right) \tag{3}$$

From Equation 3, we have a relation that describes the flow rate in terms of the resistance and can be used to calculate the specific resistance for each channel with physical parameters from the system. However, Branch 2 has a heterogenous cross section due to the step; therefore, the resistances of each section of the bypass channel must be considered to find the total resistance through Branch 2:

$$\left(\frac{\tilde{R}_1}{\tilde{R}_2}\right) = \left(\frac{\tilde{R}_1}{\tilde{R}_i + \tilde{R}_{ii} + \tilde{R}_{iii}}\right) = \left(\frac{Q_2}{Q_1}\right) \tag{4a}$$

And plugging in Equation 2:

$$\left(\frac{\mu\frac{p_1}{\lambda_1 S_1^2}L_1}{\mu\frac{p_i}{\lambda_i S_i^2}L_i + \mu\frac{p_{ii}}{\lambda_{ii} S_{ii}^2}L_{ii} + \mu\frac{p_{iii}}{\lambda_{iii} S_{iii}^2}L_{iii}}\right) = \left(\frac{Q_2}{Q_1}\right)$$

(4b)

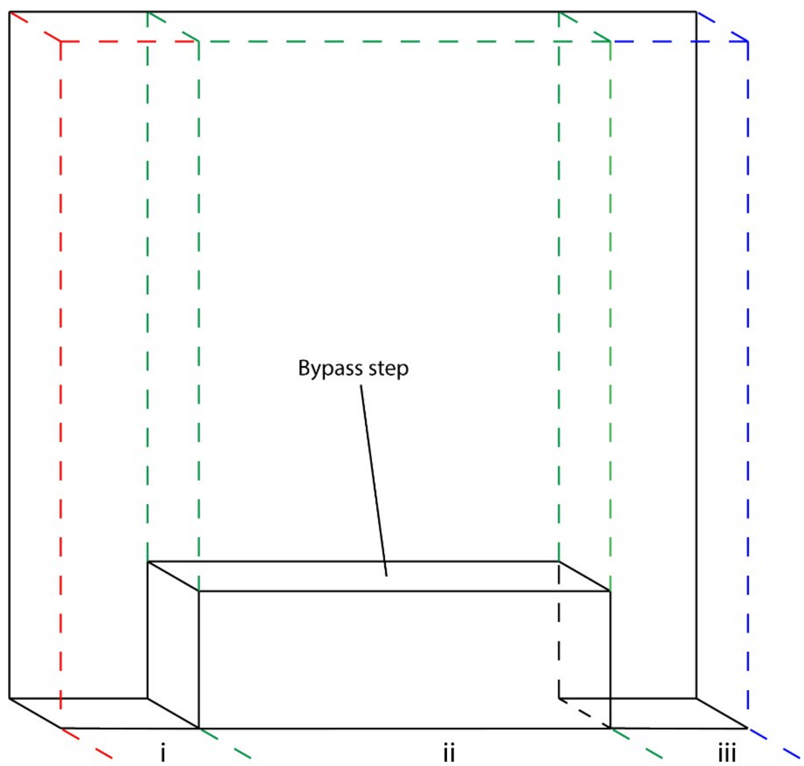

Figure S3ii: Isometric view of cross section of Branch 2 (Bypass)

Where i, ii, and iii represent the separate sections within the bypass channel (Figure S3ii). Plugging in the physical parameters into Equation 4b provides the ratio of the fluxes between the bypass channel and the main channel. For our specific stepped bypass platform:

$$\frac{Q_2}{Q_1} = 2.68$$

(5a)

And without a step in the bypass channel:

$$\frac{Q_2}{Q_1} = 3.18$$

(5b)

These calculations demonstrate that incorporation of the step into the bypass decreases the flux through the bypass by increasing the resistance through the bypass channel. The decreased flux through the bypass

(Branch 2) corresponds to an increased flux through the main channel (Branch 1), which drives the droplets completely through the curves in the channels and allows them to flow to the outlet.

References:

2. Berthier, J.; Gosselin, D.; Berthier, E. A generalization of the Lucas-Washburn Rideal law to composite microchannels of arbitrary cross section. Microfluid. Nanofluid., 2015, 19, 3, 497-507.
3. Lee, J.J.; Karampelas, I.H.; Brakke, K.A.; Theberge, A.B.; Berthier, E.; Berthier, J. Capillary flow of solvents and aqueous liquids in rounded open microgrooves. Langmuir. Accepted.

S4: Workflow for Droplet Length Measurements

To measure the length of the aqueous droplets in our channels, we designed and fabricated T junction platforms without outlet reservoirs. As with the devices with the outlet reservoir, we pipetted a 3 µL droplet upstream of the T junction and the added carrier fluid to the inlet reservoir. After initiation of spontaneous capillary flow (SCF) and splitting of the droplet, daughter droplets flowed to the end of the channel, where they stopped and were compressed as the device filled with carrier fluid. Once the device was completely filled and flow had completely ceased, the daughter droplets at the end of the channel were imaged. Images of droplets were then analyzed with ImageJ. Specifically, A-B) images were opened (symmetric droplet image) and scaled (Analyze, set scale); C) the "Segmented Line" tool was then selected and a vertical line was drawn from the top of each droplet to the bottom. D) The segmented line was measured (Analyze, measure) and droplet lengths were recorded.

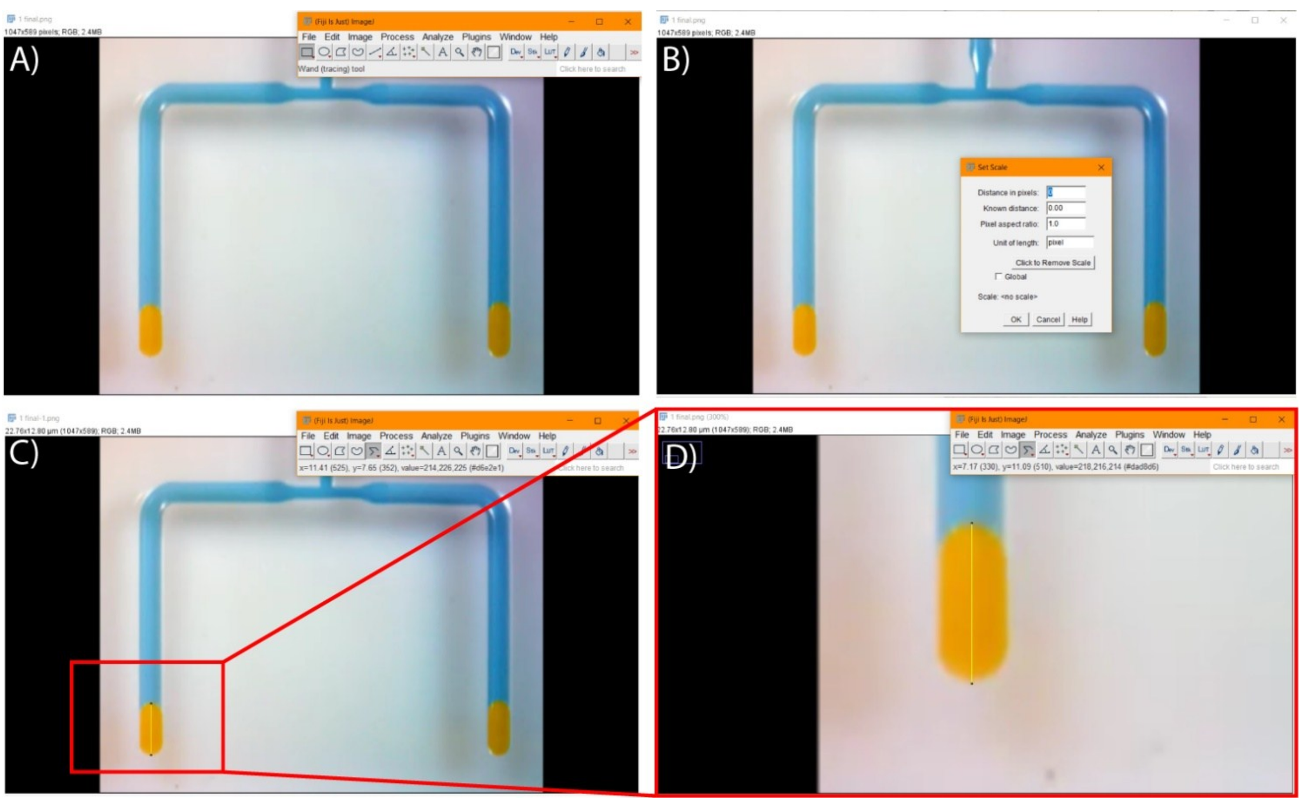

Figure S4: Workflow for droplet length measurement. A) The image to be measured is opened using ImageJ; B) to set the scale, we selected "Analyze, set scale" and changed the scale from pixels to µm; C) the Segmented Line tool is selected, and a line is draw from one end of the droplet to the other (interface of droplet and carrier phase and boundary of droplet and end of channel); D) zoomed-in image illustrating the line drawn on the droplet.

S5: Droplet splitting reproducibility within a single device

To demonstrate the reproducibility of droplet splitting within a single device, we measured the droplet area and perimeter after splitting in one device. After flowing the droplet through the 1:1 T-junction (Fig. 4B) and measuring droplet area and perimeter once it reached the outlet reservoir, the device was washed with 70% ethanol, rinsed with water, dried with compressed air, and then reused. Images were analyzed using ImageJ and the "circle" drawing tool to encapsulate the droplet prior to measurement and recording.

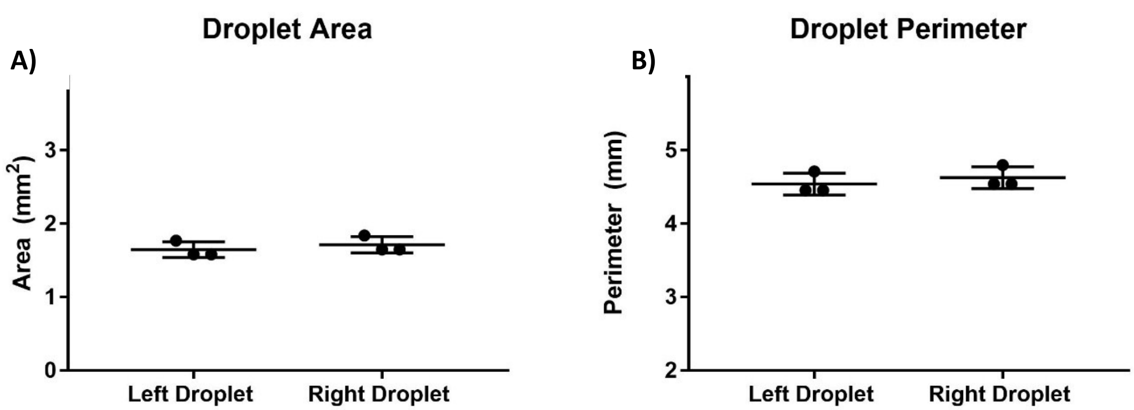

Figure S5: Reproducibility of droplet splitting within one device. Daughter droplet area (A) and perimeter (B) were measured using ImageJ for one droplet split using the 1:1 T-junction device in n=3 independent experiments. After splitting and droplet quantification, the same device was cleaned, dried, and used for the subsequent independent experiment. Mean and standard deviation are indicated for n=3 droplets across n=3 independent experiments.

S6: Table of Video Files Included in Supporting Information

Video	File Name
S1	Fig 1B Shift mode.mpg
S2	Fig 1C Raft mode.mpg

S3	Fig 2A Open channel.mpg
S4	Fig 2B Open channel with bypass.mpg
S5	Fig 2C Open channel with stepped bypass.mpg
S6	Fig 3 Array droplet system.mpg
S7	Fig 4B Symmetric droplet splitting.mpg
S8	Fig 4C Asymmetric droplet splitting.mpg
S9	Fig 5 Droplet splitting and mixing.mpg

S7: Table of Design Files Included in Supporting Information

Device Figure	File Name
Figure 1B	Open channel.STEP
Figure 2A	Open channel.STEP
Figure 2B	Open channel with bypass.STEP
Figure 2C	Open channel with stepped bypass.STEP
Figure 3	Multichannel device.STEP
Figure 4B	T junction 1-1.STEP
Figure 4C	T junction 1-2.STEP
Figure 5	T junction 1-1.STEP